

# The proton nuclear magnetic shielding tensors in biphenyl: Experiment and theory

Frank Schönborn<sup>a</sup>, Heike Schmitt<sup>a</sup>, Herbert Zimmermann<sup>a</sup>, Ulrich Haeberlen<sup>a,\*</sup>,  
Clémence Corminboeuf<sup>b</sup>, Gisbert Großmann<sup>c</sup>, Thomas Heine<sup>c,\*</sup>

<sup>a</sup> Max-Planck-Institut für Medizinische Forschung, Jahnstr. 29, 69120 Heidelberg, Germany

<sup>b</sup> Département de chimie physique, Université de Genève, CH-1211 Genève 4, Switzerland

<sup>c</sup> Institut für Physikalische Chemie und Elektrochemie, TU Dresden, 01062 Dresden, Germany

Received 3 January 2005; revised 4 March 2005

Available online 19 April 2005

## Abstract

Line-narrowing multiple pulse techniques are applied to a spherical sample crystal of biphenyl. The 10 different proton shielding tensors in this compound are determined. The accuracy level for the tensor components is 0.3 ppm. The assignment of the measured tensors to the corresponding proton sites is given careful attention. Intermolecular shielding contributions are calculated by the induced magnetic point dipole model with empirical atom and bond susceptibilities (distant neighbours) and by a new quantum chemical method (near neighbours). Subtracting the intermolecular contributions from the (correctly assigned) measured shielding tensors leads to isolated-molecule shielding tensors for which there are symmetry relations. Compliance to these relations is the criterion for the correct assignment. The success of this program indicates that intermolecular proton shielding contributions can be calculated to better than 0.5 ppm. The isolated-molecule shielding tensors obtained from experiment and calculated intermolecular contributions are compared with isolated-molecule quantum chemical results. Expressed in the icosahedral tensor representation, the rms differences of the respective tensor components are below 0.5 ppm for all proton sites in biphenyl. In the isolated molecule, the least shielded direction of all protons is the perpendicular to the molecular plane. For the *para* proton, the intermediate principal direction is along the C–H bond. It is argued that these relations also hold for the protons in the isolated benzene molecule.

© 2005 Elsevier Inc. All rights reserved.

**Keywords:** Proton shielding tensors; Intermolecular contributions; Quantum chemical calculations; Symmetry relations

## 1. Introduction

The chemical shift tensors  $\sigma$  have now been measured for protons in a substantial variety of bonding situations, mostly by applying line-narrowing multiple pulse spectroscopy [1,2] either to powder samples or, preferably, to single crystals [3]. This field of research is now closed. One task that was left behind is the determination of  $\sigma$  in benzene, i.e., in the prototype aromatic sys-

tem. In the isolated benzene molecule, the symmetry  $mm2$  of any H atom site specifies completely the orientation of the principal axes of the proton's  $\sigma$ -tensor: one must be perpendicular to the molecular plane, another parallel to the C–H bond and the third parallel to the in-plane-perpendicular-to-the-bond. The open question is which of the least, intermediate and most shielded principal components goes with which of the principal axes, and how large are the differences between these principal components. It is fairly clear that the perpendicular to the molecular plane is the least shielded direction [4–6]. However, it is not known whether the most shielded direction is parallel or perpendicular to the C–H bond and earlier attempts to resolve this question

\* Corresponding authors. Fax: +49 6221 486 351 (U. Haeberlen), +49 351 46335953 (T. Heine).

E-mail addresses: [ulrich.haeberlen@mpimf-heidelberg.mpg.de](mailto:ulrich.haeberlen@mpimf-heidelberg.mpg.de) (U. Haeberlen), [thomas.heine@chemie.tu-dresden.de](mailto:thomas.heine@chemie.tu-dresden.de) (T. Heine).

by quantum chemical methods, applied to the isolated benzene molecule [7–10], did not lead to a definitive conclusion.

In this work, we are going to clarify this question, both by experiment and theory. Actually, the measurements date back to 1996 [11]. For several reasons such as inconvenient melting point (5.5 °C), orthorhombic unit cell containing four molecules, and high molecular mobility even at liquid nitrogen temperature, benzene is not a suitable candidate for a single-crystal line-narrowing multiple pulse experiment which requires handling a spherically shaped sample of known orientation. Therefore, we concentrated our efforts on biphenyl,  $\text{H}_5\text{C}_6\text{-C}_6\text{H}_5$ , which perhaps is the closest relative to benzene. The isolated-molecule neighborhood of, in particular, the H-atoms in the *para* positions of biphenyl closely resembles that of any H-atom in benzene. Their site symmetries are the same. It is well-known that in solution the *meta* protons of substituted benzenes resonate close to the  $^1\text{H}$  benzene shift. For biphenyl, however, the situation is different, see Section 4. Hence, it is well justified to assume that the relations between principal components and principal axes of the shielding tensors of the *para* H atoms in biphenyl reflect those in benzene. Biphenyl is amenable to a line-narrowing multiple pulse experiment: its melting point (69 °C) is well above room temperature (actually, the real problem is not melting but rapid sublimation) and it crystallizes in the simpler monoclinic space group  $\text{P}2_1/\text{a}$  with two molecules in the unit cell [12]. The molecules sit on inversion centers of the crystal meaning that there are five crystallographically and 10 magnetically inequivalent hydrogen sites and hence in general 10 different resonances in the multiple pulse spectrum. The resolution of these 10 resonances is a considerable challenge. The analysis of the spectra and eventually of the rotation patterns of line positions faces a major problem: the assignment of the 10  $\sigma$ -tensors that at the end are extracted from the spectra and rotation patterns.

We will show, in particular, that the resonances from the protons in the *para* positions can be singled out. This is accomplished by exploiting a particular type of molecular motion in biphenyl, namely flips of the phenyl rings about the long molecular axis [13,14]. At a sufficiently low temperature, say  $T < -20$  °C, the rate of these flips is so low that the resonances in multiple pulse spectra are not affected by the flips. At room temperature, however, where the flip rate is in the kilohertz region [13], the resonances from the *meta* and *ortho* protons become exchange broadened while those from the protons in the *para* positions remain (fairly) narrow. This circumstance will allow us to identify the latter unequivocally. By invoking theory and symmetry arguments we shall eventually also be able to assign the other measured shielding tensors to “their” protons.

Having found the  $\sigma$ -tensor of the proton in the *para* position of biphenyl still does not answer our original question. The reason is that intermolecular shielding contributions cause the measurable  $\sigma$ -tensor to deviate significantly from that in the isolated molecule [6,15,16]. Note that, in general, the problem with intermolecular shielding contributions is particularly acute for protons because, first, protons usually sit, as they do in biphenyl, at the periphery of the molecule and are thus exposed to stronger fields arising from electron motions in neighboring molecules than nuclei located further inside such as carbons.<sup>1</sup> Second, proton shift anisotropies are intrinsically “small.” Thus, intermolecular shielding contributions, which are not tied to the molecular symmetry, can easily drive the principal axes system of the measurable  $\sigma$ -tensor significantly away from its orientation in the isolated molecule where it is possibly fixed by molecular symmetry. Thus, to answer the question about the proton shielding tensor in the isolated molecule we must invoke a necessarily theoretical access to the intermolecular shielding. This will be done in Section 5. The final result will be that for the H-atom in the *para* positions of the isolated biphenyl molecule and, very likely, for any H-atom in the isolated benzene molecule as well, the most shielded direction is the in-plane-perpendicular to the C–H bond. The in-plane shielding difference is about 2 ppm. Basically, isolated-molecule shielding of the *meta* and *ortho* protons in biphenyl shows the same characteristics. There are, however, modifications that can be traced back to the presence of the other ring.

## 2. Experimental

### 2.1. Notation

For designating the H atoms in the biphenyl molecule, see Fig. 1, we use the notation of Charbonneau and Délugeard [12,18,19], who, in a series of X-ray and neutron diffraction studies have determined the molecular and crystal structure of biphenyl. For  $T > 40$  K, the space group of the crystal is  $\text{P}2_1/\text{a}$ , at  $T = 293$  K  $a = 8.12$  Å,  $b = 5.63$  Å,  $c = 9.51$  Å, and  $\beta = 95.1^\circ$ . The molecules are located on inversion centers. The unit cell contains two molecules A and B which are related by a twofold screw axis along **b**. A is the molecule at the origin of the cell as defined in [12]. In Fig. 1 we also introduce with heavy arrows the so-called standard orthonormal axes system  $X_{\text{SOS}}$ ,  $Y_{\text{SOS}}$ ,  $Z_{\text{SOS}}$  with  $X_{\text{SOS}}\|\mathbf{a}$ ,  $Y_{\text{SOS}}\|\mathbf{b}$ , and  $Z_{\text{SOS}}\|\mathbf{c}^*$ ,  $\mathbf{c}^* = \mathbf{a} \times \mathbf{b}$  and, as well, a

<sup>1</sup> Barich et al. [17] investigated the  $^{13}\text{C}$  shielding tensors in biphenyl. They judged that intermolecular shielding contributions can be ignored.

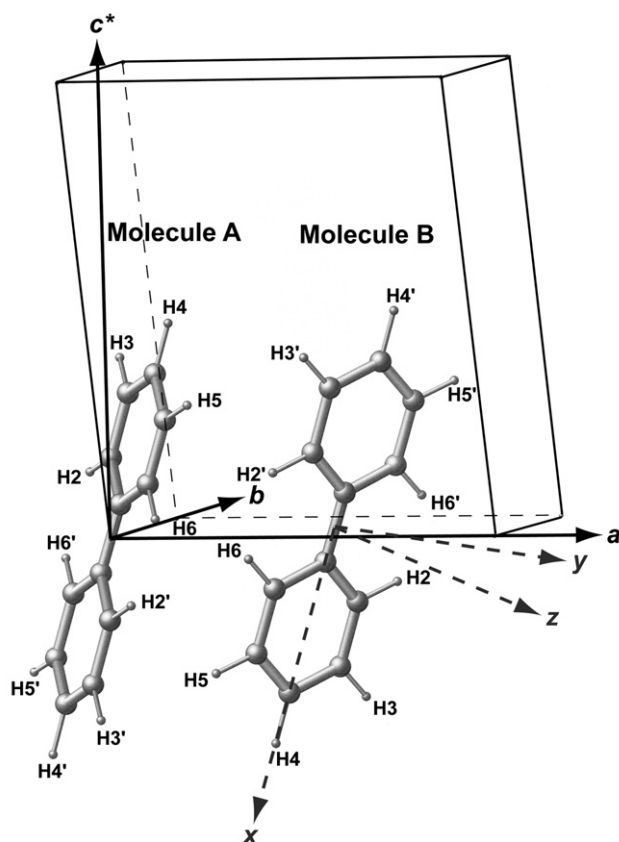


Fig. 1. The unit cell of biphenyl with molecules A and B and the labelling of the H-atoms. H2 and H6 occupy *ortho*, H3 and H5 *meta*, and H4 *para* positions. The standard orthogonal system SOS with axes along **a**, **b** and **c\*** and the molecular axes system *x*, *y*, *z* are indicated.

molecular axes system *x*, *y*, *z* whose axes are parallel to the three twofold symmetry axes of the molecule.

## 2.2. Sample preparation

After extensive zone refining of commercially obtained biphenyl, a single crystal was grown from the melt by the Bridgeman method. To avoid line broadening and line shifts from bulk susceptibility effects [4] we shaped on a lathe the as grown crystal, which was to become the sample, into an approximate sphere, see Fig. 2A. A two-piece cubic sample holder with a hollow space matching the shape of the crystal was machined of Kel-F, which is a plastic material free of hydrogens, see Fig. 2B. This cube, in turn, could be inserted into a precisely matching cubic cavity of a two-piece cylindrical rod made also of Kel-F, see Fig. 2C. The sample thus fills completely a nearly spherical cavity of a “long” homogeneous cylinder which is an arrangement that is well-known to exclude any influence of bulk sample susceptibility on NMR results apart from a common shift of all resonances which is independent of rotations about the rod axis. The rod could be rotated inside the rf coil of the NMR probe. The rotation axis is perpen-

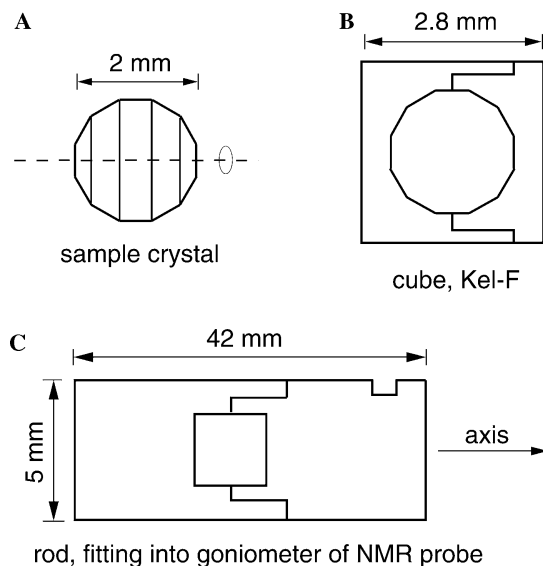


Fig. 2. Sample (A) and parts (B and C) for its mounting in the goniometer of the NMR probe. The projection of the sample crystal onto a plane containing its rotation axis is a regular dodecagon. A thin glass plate functioning as a mirror is glued in the groove at the upper right end of (C). Together with a laser beam it allowed us to set the initial rotation angle of the sample.

dicular to the applied field  $B_0$ . For setting the initial rotation angle, a small mirror was fixed in a groove of the rod, see Fig. 2C, whose orientation was monitored with a laser beam. By inserting the cube into the cavity of the rod with, in turn, the cube axes *X*, *Y*, and *Z* along the rod axis and taking multiple pulse spectra for a series of increments of the rotation angle  $\varphi$  we could explore the proton chemical shifts in three mutually orthogonal planes of the crystal.

After completing the NMR measurements, the cube was opened and, using X-rays, the orientation of the cube axes *X*, *Y*, and *Z* was measured relative to the standard orthonormal system (SOS) of the crystal. It turned out that in the SOS the polar angles  $\theta$  and  $\phi$  of the cube axes *X*, *Y*, and *Z* were

$$\theta_X = 77.1^\circ, \quad \phi_X = 144.6^\circ,$$

$$\theta_Y = 79.7^\circ, \quad \phi_Y = 236.9^\circ,$$

$$\theta_Z = 16.6^\circ, \quad \phi_Z = 4.4^\circ.$$

We use deliberately the past tense because after exposing the crystal (mind its dimensions!) to the X-rays in open air for a considerable length of time a large part of it had disappeared by sublimation.

## 2.3. Multiple-pulse NMR

The measurements reported here were done on the 270 MHz multiple-pulse spectrometer described in [20]. For line-narrowing, the BR-24 sequence [21] with

$\tau = 3 \mu\text{s}$  and pulse-duration  $t_w = 0.8 \mu\text{s}$  was used. For further experimental details (e.g., composite preparation pulse, multi-window sampling) see [22].

### 3. Quantum chemical calculations

The molecular structure of biphenyl was optimized at the B3LYP/6-31G\* level as implemented in Gaussian 98 [23]. The optimized structures were arranged in a unit cell using the intermolecular distances and molecular orientations from X-ray experiments [12]. NMR computations were performed employing the IGLO method [24] with Foster-Boys localized [25] molecular orbitals, which themselves were calculated using gradient-corrected density-functional theory [26] and the IGLO-III basis set [9] employing the deMon programs [27,28].

As the direct computation of the proton shielding in a large biphenyl cluster is not feasible at present a first-order approximation was used: the shielding tensor of a selected atom in the reference molecule is taken as the sum of the contribution of the reference molecule itself (hence, the isolated-molecule shielding tensor) plus the shielding tensors originating separately from each molecule of the crystal at the position of the selected atom in the reference molecule. This approximation is motivated by two assumptions: first, treating a molecular crystal as a superposition of isolated molecules assumes that the electronic interactions, which in this case are limited to the London type, do not influence the electronic density of the isolated molecules. Indeed, various calculations at various levels of theory for that type of interactions show that the electron densities of the isolated molecules are only slightly perturbed [29,30].

However, it is well-known that aromatic rings show a long-range induced magnetic field, which influences shielding tensors on the intermolecular scale [31]. Our second assumption is the additivity of the induced magnetic fields. The local field at the position of a proton  $\mathbf{R}$  can be written as the sum of intra- and intermolecular contributions of induced fields:

$$\mathbf{B}^{\text{loc}}(\mathbf{R}) = \mathbf{B}^{\text{ind,intra}}(\mathbf{R}) + \mathbf{B}^{\text{ind,inter}}(\mathbf{R}). \quad (1)$$

In the same vein, the corrected external field at the proton position is given by

$$\mathbf{B}^{\text{ext,correct}}(\mathbf{R}) = \mathbf{B}^{\text{ext}} + \mathbf{B}^{\text{ind,inter}}(\mathbf{R}) \approx \mathbf{B}^{\text{ext}}. \quad (2)$$

This is a good approximation as the induced field is approximately  $10^6$  times smaller than the external field, and motivates that the intramolecular contribution is the same as in vacuum

$$\mathbf{B}^{\text{ind,intra}}(\mathbf{R}) = -\boldsymbol{\sigma}(\mathbf{R}) \cdot \mathbf{B}^{\text{ext}}. \quad (3)$$

For the shielding tensor it follows that

$$\boldsymbol{\sigma}(\mathbf{R}) = \boldsymbol{\sigma}^{\text{intra}}(\mathbf{R}) + \boldsymbol{\sigma}^{\text{inter}}(\mathbf{R}). \quad (4)$$

This approximation was tested carefully for several biphenyl clusters. Details will be presented under separate cover (T. Heine, C. Corminboeuf, G. Grossmann, U. Haeberlen).

These calculated shielding tensors are, however, still subject of numerous uncertainties, including inherent approximations within the theoretical IGLO-DFT methodology, basis set incompleteness, inaccurate geometrical parameters, rovibrational contributions, etc., which may reach a magnitude which is not negligible for our purpose. Therefore, we will reduce these errors by insertion of an empirical factor scaling the quantum chemical contributions (see Section 5.3).

### 4. Results and analysis of raw data

In Fig. 3 we show a multiple pulse spectrum recorded from our biphenyl sample crystal and, for comparison, a “wide-line” and a 500 MHz liquid-state high-resolution spectrum. We do not comment the readily interpretable liquid-state spectrum except that it spans a spectral range of 0.24 ppm and that the linewidths are below 1 Hz, i.e., below 0.002 ppm. Note the fact that the shift of the *para* protons (7.35 ppm) is near the benzene shift (7.26 ppm), while the shift of the *meta* protons is 7.44 ppm. The wide-line spectrum has a width (FWHM) of about 30 kHz corresponding, at 270 MHz, to roughly 110 ppm. The width of the resonances in the multiple pulse spectrum is about 0.7 ppm, hence line-narrowing by a factor of more than 150 was achieved. The multiple pulse spectrum was recorded at  $T = 250 \text{ K}$ . It shows eight resolved lines, two of which being significantly more intense than the others. Counting these intense lines as double, we can indeed locate all 10 expected resonances. We have recorded such spectra for increments of  $3^\circ$  to  $10^\circ$  of the rotation angle  $\varphi$  with each of the  $X$ ,  $Y$ , and  $Z$  cube axes along the rod axis, and have plotted the positions of the resonances in rotation patterns, see Fig. 4. At  $T = 250 \text{ K}$ , the spin–lattice relaxation time  $T_1$  of the protons in biphenyl is roughly 35 min. To prevent drifts of the spectrometer, small as they were, to become eventually a problem, we took a spectrum every 10 min and only when the signal-to-noise ratio was judged to be too small for identifying the peaks were additional spectra recorded with waiting times of 30 or 60 min.

The variation with  $\varphi_i$ ,  $i = X, Y, Z$ , of the position  $\nu^{(p)}(\varphi_i)$  of the resonance from any proton  $p$  in the unit cell of the crystal must follow a  $K_i^{(p)} + C_i^{(p)} \cos 2\varphi_i + S_i^{(p)} \sin 2\varphi_i$  dependence [32], where  $K_i^{(p)}$ ,  $C_i^{(p)}$ , and  $S_i^{(p)}$  are constant coefficients. Indeed, the data points in each of the  $X$ ,  $Y$ , and  $Z$  rotation patterns can be connected reasonably well by 10 such curves, see again Fig. 4. These curves are actually least-squares best-fits to those data points which were identified for sure as arising from a particular proton  $p$ . With the help

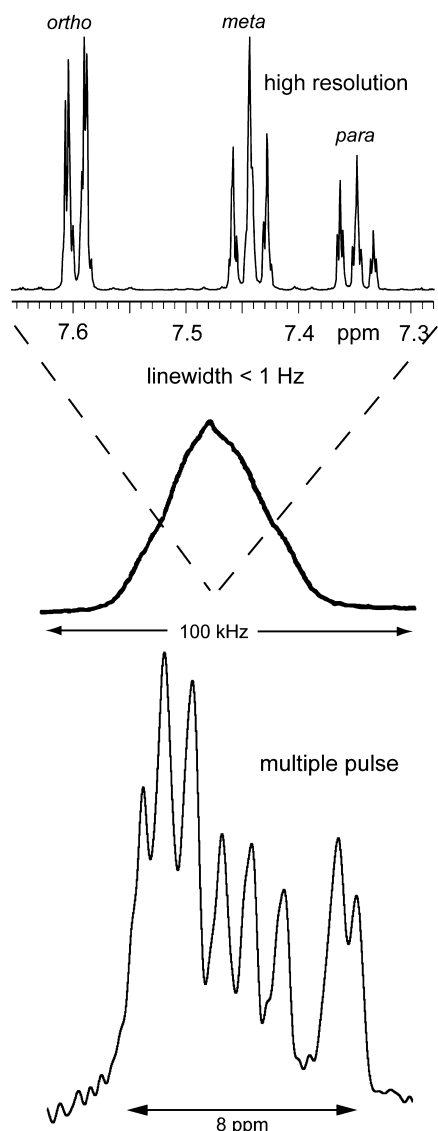


Fig. 3. A 500 MHz high resolution spectrum of biphenyl in  $\text{CDCl}_3$ , a solid-state wide line and a 270 MHz single-crystal multiple pulse spectrum. The width (FWHM) of the wide line spectrum is about 30 kHz or 110 ppm, the width of the resonances in the multiple pulse spectrum is about 0.7 ppm, i.e., line narrowing by a factor of 150 was achieved.

of the mirror referred to in Fig. 2, we adjusted the initial rotation angle such that for  $\varphi_i = 0$ ,  $i = X, Y, Z$ , the applied field  $\mathbf{B}_0$  was parallel to, respectively, the cube axis  $Y, Z$ , and  $X$ .

The direction  $\mathbf{B}_0 \parallel Y$  occurs both in the  $X$  pattern (for  $\varphi_X = 0^\circ$ ) and in the  $Z$  pattern (for  $\varphi_Z = 90^\circ$ ) and something analogous is true for  $\mathbf{B}_0 \parallel X$  and  $\mathbf{B}_0 \parallel Z$  in the  $Y$  and  $Z$ , and in the  $X$  and  $Y$  patterns, respectively. These special directions are marked in Fig. 4. They allow us to identify those curves in the three patterns that arise from one and the same proton in the unit cell.

Other special directions are where the path of  $\mathbf{B}_0(\varphi_i)$  on the unit sphere around the origin of the SOS crosses the monoclinic plane of the crystal. These directions are

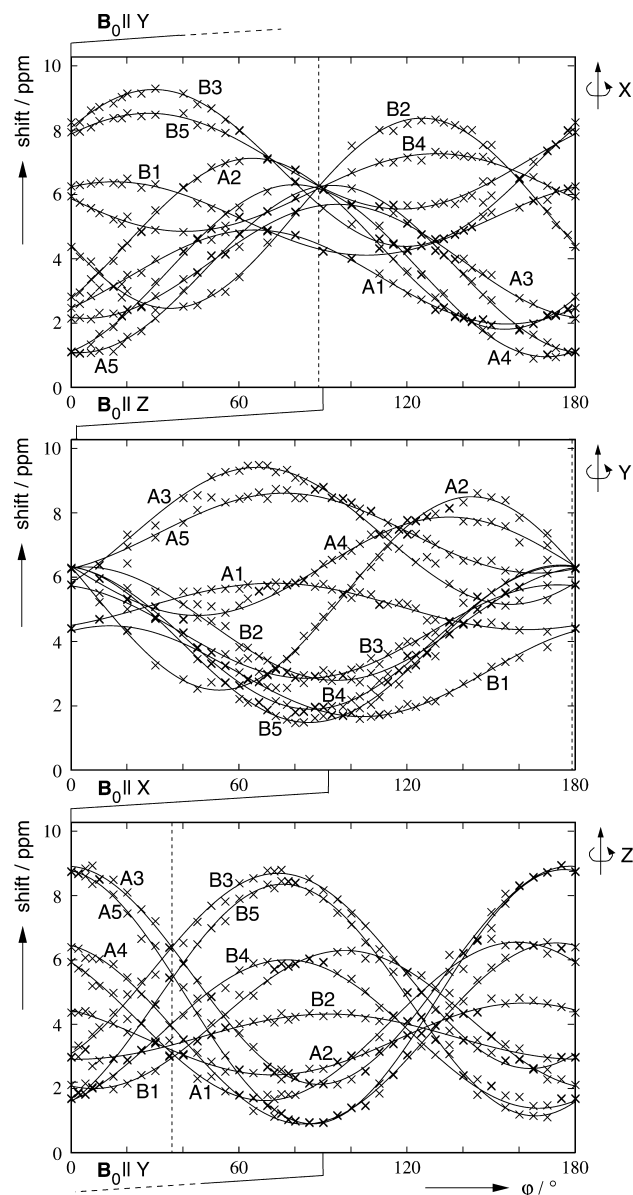


Fig. 4. Rotation patterns of line positions in multiple pulse spectra when rotating the crystal of biphenyl about the cube edges  $X, Y$ , and  $Z$ . The dotted lines indicate where the path of  $\mathbf{B}_0(\varphi_i)$ ,  $i = X, Y, Z$ , crosses the monoclinic plane. The sine curves are fits to those data points that were identified to stem from a particular H atom. See text for the labelling of the curves.

marked in Fig. 4 by vertical dotted lines. For these directions of  $\mathbf{B}_0$ , the resonances of the symmetry related protons  $A_p$  and  $B_p$  must coincide. Due to experimental uncertainties, this condition is satisfied in Fig. 4 only approximately, but still sufficiently well to allow us the identification of those pairs of curves that arise from symmetry related pairs of protons.

Next we ask whether we can distinguish those curves in Fig. 4 that arise from the protons of molecules A and B. It so happens that the normal  $\mathbf{n}_B$  to the plane of molecule B is, within  $2.4^\circ$ , parallel to the cube axis  $X$ . Previous knowledge [4,5] suggests that the shielding tensors

Table 1  
Proton shielding tensors  $\sigma^{(p)}$  in biphenyl (Reference frame: SOS)

$p$	$xx^a$	$yy$	$zz$	$xy$	$xz$	$yz$	$\langle Dev. \rangle^c$	iso <sup>d</sup>	$\vartheta^e$
1 <sup>b</sup>	$-1.61 \pm 0.17$	$0.97 \mp 0.20$	$0.64 \pm 0.03$	$-1.99 \mp 0.32$	$-0.36 \mp 0.06$	$0.30 \mp 0.33$	0.18	$-1.88 \pm 0.00$	$17.7^\circ$
2	$-0.24 \pm 0.01$	$-0.61 \mp 0.11$	$0.85 \pm 0.10$	$-1.68 \mp 0.28$	$1.89 \mp 0.02$	$-2.52 \mp 0.32$	0.14	$-1.57 \mp 0.01$	$60.6^\circ$
3	$0.15 \pm 0.16$	$-0.88 \mp 0.18$	$0.73 \pm 0.02$	$-2.52 \mp 0.21$	$-1.02 \mp 0.07$	$2.34 \mp 0.31$	0.16	$-0.49 \mp 0.01$	$17.4^\circ$
4	$0.09 \pm 0.01$	$-1.14 \mp 0.11$	$1.04 \pm 0.09$	$-2.73 \mp 0.31$	$1.32 \mp 0.05$	$-0.45 \mp 0.29$	0.14	$-1.49 \pm 0.03$	$16.3^\circ$
5	$0.06 \pm 0.22$	$-1.18 \mp 0.13$	$1.12 \mp 0.09$	$-3.25 \mp 0.17$	$-0.04 \pm 0.00$	$1.91 \mp 0.26$	0.15	$-0.81 \pm 0.03$	$17.9^\circ$

<sup>a</sup> Components of traceless symmetric constituent of  $\sigma$  in ppm. The upper/lower sign gives the immediate experimental result for molecule A/B. For B the sign of the  $xy$  and  $yz$  components must be inverted.

<sup>b</sup> Label as in Fig. 4. According to final assignment: 1 $\hat{=}$ H4, 2 $\hat{=}$ H3, 3 $\hat{=}$ H5, 4 $\hat{=}$ H6, 5 $\hat{=}$ H2.

<sup>c</sup>  $\langle Dev. \rangle$  is the mean of the magnitude of the differences of the five A or B tensor components from their A/B mean.

<sup>d</sup> Isotropic shielding relative to a spherical sample of H<sub>2</sub>O.

<sup>e</sup> Deviation of least shielded principal direction from normal of molecular plane.

of all protons of B have their least shielded directions near  $n_B$ , that is, near  $X$ . Indeed, for  $B_0 \parallel X$  ( $\varphi_Y = 90^\circ$  in the  $Y$ -pattern and  $\varphi_Z = 0^\circ$  in the  $Z$  pattern) five of the curves are near their minimum. We thus propose that these curves and the associated tensors must be assigned to molecule B. The angular distance between  $Y$  and  $n_A$  is  $23.5^\circ$  which again is “small.” Hence, we expect, and find indeed, the minima of the five other curves near  $B_0 \parallel Y$ . These curves are proposed to arise from molecule A. Following these arguments we have labelled the curves in Fig. 4 A1 and B1, etc.

We are now ready to determine the 10 different proton shielding tensors  $\sigma^{(p)}$  in biphenyl (symmetric constituents only). Because, from the fitting procedure mentioned above, we know the coefficients  $K_i^{(p)}$ ,  $C_i^{(p)}$ , and  $S_i^{(p)}$ , it is best to base the analysis on these coefficients. It is most easily carried out in the cube axes system CAS with axes  $X$ ,  $Y$ , and  $Z$ . Due to the special choice of the initial rotation angles, the component  $\sigma_{XX}^{(p)}$  of a tensor  $\sigma_{CAS}^{(p)}$  is simply given by  $K_Z^{(p)} + C_Z^{(p)}$  and by  $K_Y^{(p)} - C_Y^{(p)}$  as well.  $K_Z^{(p)} + C_Z^{(p)}$  will usually not be *exactly* equal to  $K_Y^{(p)} - C_Y^{(p)}$ , therefore we take their *mean* for  $\sigma_{XX}^{(p)}$ . Analogous relations yield the other diagonal components  $\sigma_{YY}^{(p)}$  and  $\sigma_{ZZ}^{(p)}$ . The off-diagonal components  $\sigma_{XY}^{(p)}$ ,  $\sigma_{XZ}^{(p)}$ , and  $\sigma_{YZ}^{(p)}$  are immediately given by the coefficients  $S_Z^{(p)}$ ,  $S_Y^{(p)}$  and  $S_X^{(p)}$ , respectively. Simple enough.

In the cube axis system, the relationship between two tensors  $\sigma^{(Ap)}$  and  $\sigma^{(Bp)}$  is not easily seen, therefore we next transform the 10 tensors  $\sigma_{CAS}^{(p)}$  into the standard orthogonal system SOS where this relationship is obvious: the diagonal and  $xz$  components of  $\sigma_{SOS}^{(Ap)}$  and  $\sigma_{SOS}^{(Bp)}$  must be equal while the  $xy$  and  $yz$  components must be equal in magnitude but opposite in sign. The transformation matrix  $S$  in  $\sigma_{SOS} = S * \sigma_{CAS} * S^{-1}$  follows from the measured directions of  $X$ ,  $Y$ , and  $Z$  in the SOS and reads

$$S = \begin{pmatrix} -0.7930 & -0.5384 & 0.2852 \\ 0.5669 & -0.8235 & 0.0216 \\ 0.2233 & 0.1788 & 0.9582 \end{pmatrix}.$$

The tensors  $\sigma_{SOS}^{(Ap)}$  and  $\sigma_{SOS}^{(Bp)}$  are presented in Table 1 in a compact form. The numbers in that table are the *averages* obtained from the A and B molecules, the signs of the  $xy$  and  $yz$  components are adapted to the A molecule. The original A and B tensor components can be recovered by applying the upper and lower signs, respectively, and remembering that the signs of the  $xy$  and  $yz$  tensor components must be inverted for the B molecule. Thus, the numbers after the  $\pm$  or  $\mp$  signs express directly how well—or how poorly—a pair of  $\sigma^{(Ap)}$  and  $\sigma^{(Bp)}$  tensors obeys the relations imposed by the monoclinic symmetry of the crystal. In view of the frequent overlap of resonances and the limited resolution of the spectra that had to be analysed we think that the fulfillment of the crystal symmetry requirements is quite good. Note already at this point that the total range of isotropic shifts is 1.4 ppm, i.e., almost six times bigger than in the liquid state spectrum.

What remains is the assignment of the tensors in Table 1 to the proton sites H2, ..., H6. This is a nontrivial task and is the main subject of the following section.

## 5. Assignment and discussion

### 5.1. Overview

For assigning the measured shielding tensors  $\sigma^{(p)}$  in Table 1 to the protons  $k = H2, \dots, H6$  in the biphenyl molecule we draw on two sources of information. The first is an experimental one. It exploits the known fact that in the crystal the rings of the biphenyl molecules undergo thermally activated  $180^\circ$  flips [13,14]. In this process, the two *ortho* protons H2 and H6, and likewise the two *meta* protons H3 and H5 are exchanged while the *para* proton H4 remains unaffected. This will allow us to identify uniquely the resonances, actually 1A and 1B, from the *para* protons of molecules A and B and thus to assign the respective tensors. The exchange of the *ortho* and of the *meta* protons will lead to a constraint for the assignment of the associated tensors.

The second source of information is theory and combines two ideas. The first is that the intermolecular shielding contributions, to be called  $\sigma_{\text{inter}}^{(k)}$ , can be assessed quite efficiently by combining the results of quantum chemical shielding calculations with those of a simple model of magnetic field induced point dipoles [33,6]. The second idea is the firm knowledge that the shielding tensors in the *isolated* molecule, to be called  $\sigma_{i,m}^{(k)}$ , must obey a number of symmetry relations. These relations are most easily expressed in the molecular axes system  $x, y, z$  introduced in the caption of Fig. 1. One principal axis, actually the least shielded one, of all  $\sigma_{i,m}^{(k)}$  must be parallel to  $z$ . For the *para* proton H4, another principal axis must be parallel to  $x$ . A  $180^\circ$  rotation about  $x$  must transform  $\sigma_{i,m}^{(H2)}$  into  $\sigma_{i,m}^{(H6)}$  and likewise  $\sigma_{i,m}^{(H3)}$  into  $\sigma_{i,m}^{(H5)}$ . The isolated molecule isotropic shifts of H2 and H6, and of H3 and H5 must be equal.

By calculating the tensors  $\sigma_{\text{inter}}^{(k)}$  (they all turn out to be significantly different from each other, see below) and subtracting this set of tensors  $\{\sigma_{\text{inter}}^{(k)}\}$  from the set of measured tensors  $\sigma^{(p)}$ , and from all permutations of this latter set, we obtain sets of trial tensors  $\{\sigma_{i,m}^{(k)}\}$  which we may test for compliance with the isolated molecule symmetry relations. It will turn out that considering the isotropic shifts alone will allow us to pick out one particular permutation that represents the by far most likely correct assignment. The isolated-molecule symmetry relations pertaining to the traceless anisotropic constituent of the shielding tensors may then serve as a (stringent) test of the proposed assignment and, as well, of the trustworthiness of our way of calculating intermolecular shielding contributions.

### 5.2. Experimental clues for assignment

Here, we shall draw on the familiar spectral scenario of exchanging nuclei, namely broadening  $\rightarrow$  coalescing  $\rightarrow$  narrowing of resonances as the exchange rate increases. We do this very cautiously, i.e., we exploit only the coarsest spectral features because in multiple pulse spectroscopy this scenario is affected by the temporal structure of the applied rf irradiation [34]. In Fig. 5 we show spectra recorded at four different temperatures between 249 and 297 K. The crystal orientation was always that corresponding to  $\varphi = 17^\circ$  in the  $X$  pattern of Fig. 4. The labelling of the peaks is indicated in the 249 K spectrum. At this temperature the rate of the phenyl ring flips is about  $4 \text{ s}^{-1}$  while at 297 K it is  $1700 \text{ s}^{-1}$  [13]. When the sample temperature is increased, some of the peaks obviously broaden and eventually disappear (e.g., B3, B4, and B5) while others evolve into coalesced, exchange-narrowed peaks (e.g., that at 0.8 ppm in the 297 K spectrum) and still another simply remains, namely B1. We therefore conclude that peak B1 stems from the *para* proton of molecule B.

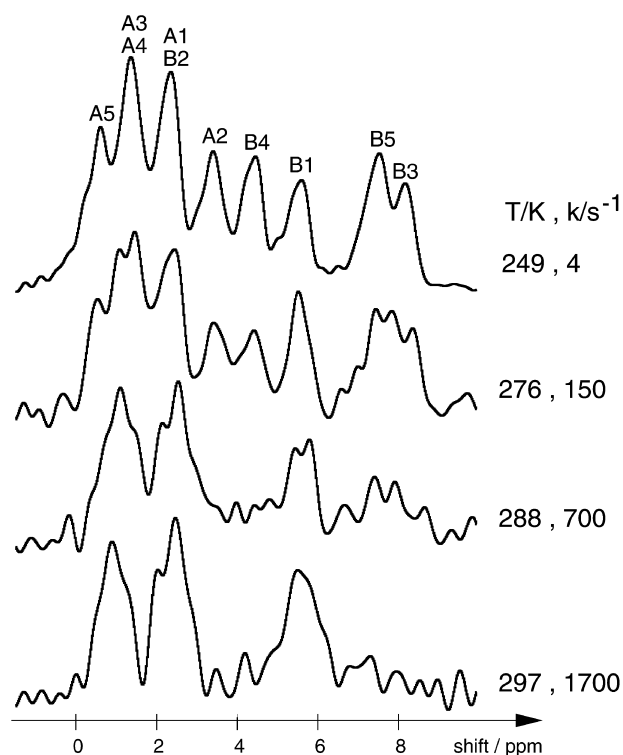


Fig. 5. Dependence of the multiple pulse spectrum of single crystal of biphenyl (rotation about  $X$ ,  $\varphi \approx 17^\circ$ ) on the temperature  $T$  or, equivalently, on the fliprate  $k$  of the phenyl rings. See text for discussion.

Then A1, which in the 249 K spectrum is overlapping with B2, must stem from the *para* proton of molecule A. This is consistent with the  $T = 276, 288,$  and  $297 \text{ K}$  spectra in Fig. 5. Because B3 and B5, despite their small chemical shift difference, do not evolve into an exchange narrowed common peak, we conclude that B3 and B5, and consequently also A3 and A5, cannot both stem from *ortho* or *meta* protons. This means that the exchange narrowed peak at about 0.8 ppm in the 297 K spectrum must have evolved from A5 and A4 implying that these peaks must both stem from either *ortho* or *meta* protons. The peak at 2.4 ppm in the 297 K spectrum is too intense to stem only from A1. There must also be a contribution from a coalesced pair of low-temperature peaks. The only possible candidates are A2 and A3 which then must stem from either *meta* or *ortho* protons.

Dropping the labels A and B and switching from speaking about (low-temperature) peaks to corresponding shielding tensors, we may summarize the findings reached so far as follows: tensor 1 must be assigned to the *para* proton H4 while tensors 2 and 3, and likewise tensors 4 and 5 must both be assigned to the *meta* protons H3 and H5 or to the *ortho* protons H2 and H6. This reduces the number of possible assignments from initially  $5! = 120$  to 8. As mentioned, any further reduction requires invoking theoretical arguments.

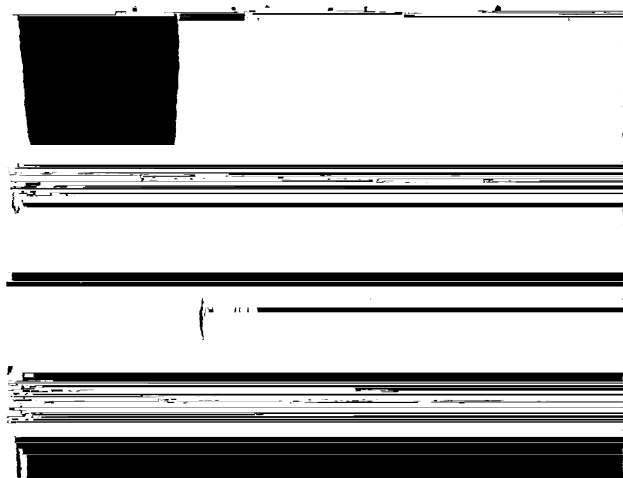


Fig. 6. Location and size of the 47 atom and bond susceptibilities in biphenyl according to Blustin [35]. The indices  $x$ ,  $y$ , and  $z$  refer to the molecular axes system introduced in Fig. 1.

### 5.3. Intermolecular shielding contributions

An excellent approximation for the contribution  $\sigma^{(j,k)}$  of a distant molecule  $j$  to the shielding of a nucleus  $k$  is [33,6]

$$\sigma^{(j,k)} = \frac{1}{4\pi R_{jk}^3} [\chi^{(j)} - 3(\mathbf{r}_{jk} \cdot \chi^{(j)}) * \mathbf{r}_{jk}]. \quad (5)$$

where  $\chi^{(j)}$  is the molecular susceptibility tensor introduced in rational units of the MKSA system, and  $R_{jk} = |\mathbf{R}_{jk}|$  is the distance from nucleus  $k$  to molecule  $j$ ;  $\mathbf{r}_{jk} = \mathbf{R}_{jk}/R_{jk}$ . The star indicates a tensor product.<sup>2</sup>

If  $R_{jk}$  is not large compared with the size of the molecule  $j$ , the applicability of Eq. (5) becomes questionable. In these situations we follow Blustin's procedure [35], i.e., we artificially break up the total molecular susceptibility into atom and bond contributions as shown in Fig. 6 and use Eq. (5) for each contribution separately.

For the very closest contacts even this procedure fails and we must resort to the full machinery of quantum chemistry. In biphenyl, such dangerously close contacts occur, e.g., between the *ortho* and *meta* protons on one side of the B molecule at the lattice position  $\frac{1}{2}, \frac{1}{2}, 0$  and the A molecule at  $0, 0, 0$  (see Fig. 1). By inversion symmetry, the same kind of contacts occur for the protons on the other side of this B molecule with the A molecule at  $1, 1, 0$ . To give an example, we choose proton  $k = \text{H2}$  (of mole-

cule B at  $\frac{1}{2}, \frac{1}{2}, 0$ ) and  $j = \text{molecule A at } 0, 0, 0$ . In the SOS the quantum chemical calculation gives for the  $xx$ ,  $yy$ ,  $zz$ ,  $xy$ ,  $xz$ ,  $yz$  components of  $\sigma^{(j,k)}/\text{ppm}$  the set of numbers  $\{6.04, 0.66, -0.33, 3.60, -1.30, -0.68\}$ ,

while the result from Eq. (5) with atom and bond susceptibilities as in Fig. 6 is

$$\{4.41, -0.07, -0.70, 2.69, -0.46, -0.70\}.$$

The largest difference occurs in the  $xx$  component, it amounts to 1.63 ppm. On the level of accuracy on which we must insist to find the correct assignment, the difference of the two sets is thus highly meaningful. One may ask, how do we know which set is better? Our answer is twofold: first, the more involved quantum chemical method *should* produce better results, second, taking this choice, we eventually can report success in terms of the tests explained under *Overview*. For large distances  $R_{jk}$  the quantum chemical results should converge to those from Eq. (5). After all, the physical idea behind Eq. (5) is sound. We consider again an example and choose  $k = \text{H2}$  of B at  $\frac{1}{2}, \frac{1}{2}, 0$  and  $j = \text{B at } \frac{1}{2}, \frac{1}{2}, 1$ . The quantum chemical result for  $\sigma^{(j,k)}/\text{ppm}$  is

$$\{-0.510, -0.255, 0.581, 0.091, -0.247, 0.343\},$$

while that from Eq. (5) is

$$\{-0.442, -0.220, 0.509, 0.081, -0.226, 0.306\}.$$

Note, first, how similar these two sets of numbers are and, second, that the numbers in the former set are systematically somewhat larger in magnitude than those in the latter. This finding is not specific to the chosen example. Because we use Eq. (5) together with atom and bond susceptibilities that add up to the experimentally measured molecular susceptibility tensor [36], we think that the intermolecular shielding contributions obtained by the quantum chemical method should be scaled such that for large distances  $R_{jk}$  they match those from Eq. (5). The optimum scale factor turns out to be  $S = 0.87$ . The need for scaling the quantum chemical shielding contributions to smaller values may arise from molecular librations and vibrations within the crystal which have been discussed earlier [12,14,17], and also from errors of the theoretical methodology, including basis set incompleteness. We emphasize, however, that, while  $S$  is comfortably close to one, scaling is an important aspect of our work since it offers the possibility to decrease the errors resulting from the mentioned uncertainties and from the influence of non-considered phenomena.

We are now ready to formulate a recipe for estimating the intermolecular proton shielding contributions  $\sigma_{\text{inter}}^{(k)}$  in biphenyl.

*Step 1.* Calculate, using the involved quantum chemical method, the intermolecular shielding contributions for a small cluster. The cluster we chose is a

<sup>2</sup> The second term in Eq. (5) derives from the second term in the expression for the magnetic field  $\mathbf{B}(\mathbf{R}) = (1/4\pi\mu_0 R^3)[\mathbf{m} - 3(\mathbf{m} \cdot \mathbf{r})\mathbf{r}]$  of a point dipole  $\mathbf{m}$  located at the origin. Because the scalar product is commutative, it is not clear to us whether the second term in Eq. (5) must be written as in the text or, alternatively, as  $\mathbf{r}_{jk} * (\chi^{(j)} \cdot \mathbf{r}_{jk})$ . The two alternatives make no difference for the symmetric constituent of  $\sigma^{(j,k)}$ , in which we are primarily interested here, they lead, however, to different *signs* of the antisymmetric constituent.

parallelepiped consisting of 27 unit cells, i.e., 54 molecules, obtained by letting the Miller indices  $h, k, l$  all run from  $-1$  to  $+1$ . Molecule B in cell  $0, 0, 0$  is the one that carries the protons  $k$ . Call the results  $\sigma_{\text{ep}}^{(k)}$ . The index ep stands for (parallel) epiped. Note that even after scaling,  $\sigma_{\text{ep}}^{(k)}$  cannot be identified with the total intermolecular shielding because the shape of the cluster is not yet right. It must be a sphere [6]. Therefore, we proceed with

*Step 2.* Repeat step 1 but use Eq. (5). Call the results  $\tilde{\sigma}_{\text{ep}}^{(k)}$ .

*Step 3.* Calculate, using again Eq. (5), the intermolecular shielding  $\tilde{\sigma}_{\text{sphere}}^{(k)}$  in a large sphere. We chose a sphere with radius  $R = 88 \text{ \AA}$ , the inversion center of molecule B in cell  $0, 0, 0$  was chosen as center of the sphere. This radius is large enough to keep the cut-off and round-off errors below 0.02 ppm which is more than sufficient. Atom and bond susceptibilities were used for  $R_{jk} \leq 44 \text{ \AA}$ , while for  $44 \text{ \AA} < R_{jk} \leq 88 \text{ \AA}$  the total molecular susceptibilities were used. It turns out, as it must indeed, that the differences  $\tilde{\sigma}_{\text{diff}}^{(k)} = \tilde{\sigma}_{\text{sphere}}^{(k)} - \tilde{\sigma}_{\text{ep}}^{(k)}$  depend only very little on  $k$ . Their average is

$$\langle \tilde{\sigma}_{\text{diff}}^{(k)} \rangle = \{-0.68, 1.37, -0.72, -0.15, 0.28, 0.08\}$$

and reflects nicely what is missing if, instead done for a sphere, the calculation is restricted to a flat parallelepiped. We now propose that  $\sigma_{\text{inter}}^{(k)}$  can be obtained from

$$\sigma_{\text{inter}}^{(k)} = \sigma_{\text{ep}}^{(k)} \cdot S + \left( \tilde{\sigma}_{\text{sphere}}^{(k)} - \tilde{\sigma}_{\text{ep}}^{(k)} \right). \quad (6)$$

The  $\sigma_{\text{inter}}^{(k)}$  so obtained are listed in Table 2. Note that the intermolecular isotropic shielding contribution for the *para* proton is quite small while those for the *meta* and *ortho* protons are much larger and, what is very important, unequal within the pairs H3/H5 and H2/H6. This tendency is already visible in the intermediate results  $\tilde{\sigma}_{\text{ep}}^{(k)}$ ,  $\sigma_{\text{ep}}^{(k)}$ , and  $\tilde{\sigma}_{\text{sphere}}^{(k)}$ .

#### 5.4. Assignment of meta and ortho proton shielding tensors

We consider the isolated-molecule isotropic shieldings obtained by subtracting the set of isotropic shieldings

of the tensors  $\{\sigma_{\text{inter}}^{(k)}\}$  from the set of isotropic values of the measured tensors  $\{\sigma^{(p)}\}$ , and from all permutations of this latter set. The measured tensor  $p = 1$  has already been assigned to the *para* proton H4, see Section 5.2. The isolated-molecule isotropic shielding of H4 relative to  $\text{H}_2\text{O}$  is  $-1.88 - 0.20 = -2.08$  ppm. If we assign the tensors  $p = 2, 3, 4$ , and 5 in this sequence to the sites  $k = \text{H3, H5, H6, and H2}$  we find that the difference of the isolated-molecule isotropic shielding of the two *meta* and of the two *ortho* protons turns out to be, respectively, 0.06 and 0.05 ppm, i.e., very small. Equality of the two *meta* and *ortho* isotropic shieldings has been one of our criteria for the correct assignment. This criterium is definitely satisfied for the assignment given here. The second-best assignment (permutation of the tensors  $p$ ) leads to shielding differences of the *meta* and the *ortho* protons of, respectively, 0.46 and 0.35 ppm, i.e., seven times bigger (worse). For the other six candidate permutations, at least one of these differences exceeds 1.4 ppm. We thus claim that the assignment shown above is the correct one. Note that it satisfies the constraint developed in Section 5.2.

The most urgent question to be asked now is: do the traceless anisotropic constituents of the isolated-molecule tensors

$$\sigma_{i.m.}^{(k)} = \sigma^{(p)} - \sigma_{\text{inter}}^{(k)} \quad (7)$$

with  $p$  related to  $k$  as shown above fulfill the symmetry relations discussed under *Overview*? Remember, the answer is a crucial test of our experimental *and* of our intermolecular theoretical shielding results, and, in addition, of the assignment based on the isotropic shieldings.

To answer this question we present in Table 3 the  $\sigma_{i.m.}^{(k)}$ , expressed in the molecular axis system  $x, y, z$ . First, consider the deviations  $\vartheta_{i.m.}^{(k)}$  of the least shielded principal directions from  $z$ , i.e., from the perpendicular of the molecular plane. Ideally, these deviations should be zero. Our data analysis cranks them out as remarkably small, see Table 3, second last column. Note how much larger these angles are for the measured tensors, cf. column  $\vartheta$  in Table 1. This means that also the symmetry requirement discussed here is definitely met satisfactorily.

We now turn to the in-plane properties of the  $\sigma_{i.m.}^{(k)}$  to clarify whether the most shielded or the intermediate

Table 2

Intermolecular shielding contributions<sup>a</sup>  $\sigma_{\text{inter}}^{(k)}$  obtained by Eq. (6) (Reference frame: SOS)

$k$ , site	$xx$	$yy$	$zz$	$xy$	$xz$	$yz$	iso
H4', <i>para</i>	-0.04	0.41	0.23	-0.70	-0.85	0.46	0.20
H3', <i>meta</i>	1.92	0.48	-0.30	-0.64	-0.11	1.96	0.70
H5', <i>meta</i>	3.83	1.49	0.20	1.03	-1.68	-0.79	1.84
H2', <i>ortho</i>	5.22	2.28	-0.90	1.03	-1.65	0.01	2.20
H6', <i>ortho</i>	3.54	1.56	-0.69	-0.03	-1.64	-0.04	1.47

<sup>a</sup> The reference molecule is B, see Fig. 1. Listed are the components of the symmetric constituent of the shielding tensor contribution in ppm and the isotropic shielding contribution.

Table 3

Isotropic shieldings and traceless shielding tensors  $\sigma_{i,m}^{(k)}$  in isolated biphenyl molecule obtained from Eq. (7) and by the quantum chemical method,  $\sigma_{q,ch}^{(k)}$  (Reference frame: molecular axes system)

$k$ , site		iso	xx	yy	zz	xy	xz	yz	$\vartheta^c$	$\varepsilon^d$
H4, <i>para</i>	$\sigma_{i,m}$	-2.08 <sup>a</sup>	0.71	2.65	-3.36	0.01	0.11	0.04	1.6°	0.2°
	$\sigma_{q,ch}$	23.10 <sup>b</sup>	0.13	2.87	-3.00	0.01	0.0	0.0	0.0°	-0.2°
H3, <i>meta</i>	$\sigma_{i,m}$	-2.27	2.72	0.89	-3.61	-1.39	0.00	-0.08	1.1°	1.7°
	$\sigma_{q,ch}$	22.98	2.73	0.64	-3.37	-1.27	0.0	0.0	0.0°	4.0°
H5, <i>meta</i>	$\sigma_{i,m}$	-2.33	2.35	0.83	-3.18	1.24	-0.12	0.10	2.5°	0.8°
	$\sigma_{q,ch}$	22.98	2.73	0.63	-3.36	1.28	0.0	0.0	0.0°	-4.0°
H2, <i>ortho</i>	$\sigma_{i,m}$	-3.01	4.47	0.64	-5.11	1.41	-0.20	0.09	1.9°	-11.9°
	$\sigma_{q,ch}$	22.21	5.32	-0.19	-5.13	1.67	0.0	0.0	0.0°	-12.4°
H6, <i>ortho</i>	$\sigma_{i,m}$	-2.96	4.44	0.43	-4.87	-1.57	-0.23	0.06	1.4°	11.0°
	$\sigma_{q,ch}$	22.22	5.35	-0.18	-5.18	-1.73	0.0	0.0	0.0°	12.0°

<sup>a</sup> Relative to a spherical sample of H<sub>2</sub>O in ppm.

<sup>b</sup> Absolute isotropic shielding in ppm.

<sup>c</sup> Deviation of least shielded principal direction from perpendicular to molecular plane.

<sup>d</sup> Deviation of intermediate principal direction from C–H bond.

shielded principal direction is parallel to the C–H bond. The deviations  $\varepsilon_{i,m}$  in the last column in Table 3 give an unambiguous answer: the *intermediate* shielded principal direction is parallel to the C–H bond. In the left part of Fig. 7 we show the relations of the in-plane principal axes of the  $\sigma_{i,m}^{(k)}$  relative to the C–H bonds. This figure reflects in an impressive manner how well the isolated-molecule symmetry relations have worked out in this data analysis. For the *para* proton,  $\varepsilon_{i,m}$  is only 0.2° (ideally zero). For the *meta* protons there is a minute but perhaps already significant deviation of the intermediate principal axis from the bond direction. By contrast, for the *ortho* protons H2 and H6 these principal axes deviate strongly from the C–H directions, but they do it in a perfectly symmetric way!

As part of our theoretical efforts we have—of course—also *calculated* the isolated-molecule proton shielding tensors by first principle methods, see also Table 3. We denote them by  $\sigma_{q,ch}^{(k)}$  to avoid confusion with their mixed experimental/intermolecular-theoretical counterparts  $\sigma_{i,m}^{(k)}$ , which we have discussed so far. A first general observation is that the  $\sigma_{i,m}^{(k)}$  and the  $\sigma_{q,ch}^{(k)}$  agree impressively well. This gives credit, we think, to the quantum chemical method applied. The  $\sigma_{q,ch}^{(k)}$  obey the quoted symmetry relations automatically, therefore it is sufficient to restrict attention to H2, H3, and H4. In Table 4 and with Fig. 7 we compare the theoretical results with those reached in the analysis of the experimental data. In the case of the *meta* and *ortho* protons we have averaged the values of H3 and H5 and of H2

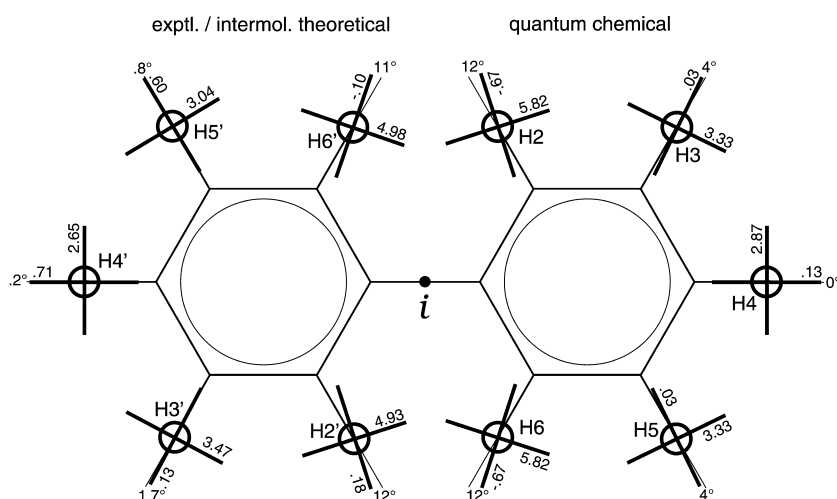


Fig. 7. Visualization of the in-plane proton shielding in the isolated biphenyl molecule. Left, from experiment and calculated intermolecular shielding contributions; right, from isolated-molecule quantum chemical calculation. The cross on each H atom indicates the directions of the intermediate and the most shielded principal axes, the numbers on the axes give the respective principal components (in units of ppm) of the traceless part of the shielding tensor. The least shielded principal axis of all protons is perpendicular to the molecular plane.

Table 4

Isotropic shieldings, traceless principal components and traceless icosahedral tensor representation of isolated-molecule proton shielding tensors  $\sigma_{i,m}^{(k)}$  and  $\sigma_{q,ch}^{(k)}$ .

Site	Method	Iso <sup>a</sup>	Principal components			Icosahedral tensor representation <sup>b</sup>						rms distance <sup>c</sup>
			11	22	33	$\sigma_1$	$\sigma_2$	$\sigma_3$	$\sigma_4$	$\sigma_5$	$\sigma_6$	
<i>para</i>	i.m.	0.00	−3.36	0.71	2.65	1.26	1.24	1.03	0.95	−2.33	−2.14	0.27
	q.ch.	0.00	−3.00	0.13	2.87	0.90	0.88	1.25	1.25	−2.14	−2.14	
<i>meta</i>	i.m.	−0.22	−3.40	0.14	3.26	0.90	3.25	−0.40	−0.24	−1.70	−1.81	0.13
	q.ch.	−0.28	−3.37	0.03	3.33	1.01	3.29	−0.47	−0.47	−1.68	−1.68	
<i>ortho</i>	i.m.	−0.90	−5.00	0.04	4.96	4.70	2.04	−0.98	−1.01	−2.19	−2.57	0.45
	q.ch.	−0.88	−5.16	−0.67	5.82	5.33	2.29	−1.56	−1.56	−2.25	−2.25	

<sup>a</sup> Isotropic shieldings referenced to  $\sigma_{iso}$  (*para*).

<sup>b</sup> Reference frame: molecular axes system.

<sup>c</sup> See Eq. (8).

and H6, respectively. The average difference between the principal components of the  $\sigma_{i,m}^{(k)}$  and  $\sigma_{q,ch}^{(k)}$  is only 0.34 ppm. The agreement of the isotropic shieldings is even much better, see third column of Table 4.

Recall that the solution-state isotropic shift difference between the *para* and *ortho* protons is 0.24 ppm, see Fig. 3. Both theory and solid-state experiment agree in that the isolated-molecule shielding difference of these protons is almost four times bigger. That their solution-state isotropic shift difference is so small is probably a result of the interaction of the biphenyl molecules with the molecules of the solvent, CDCl<sub>3</sub>, and also of the different rovibrational contributions with respect to the solid.

The cartesian tensors discussed so far contain full information about the shielding anisotropy. To appreciate the similarity of the  $\sigma_{i,m}^{(k)}$  and the  $\sigma_{q,ch}^{(k)}$ , it is not meaningful, however, to consider the rms difference of the six cartesian tensor elements because the character of the three diagonal elements is different from that of the three off-diagonal elements. The icosahedral tensor representation introduced by Alderman, Sherwood and Grant [37] circumvents this problem and works equally well in any coordinate frame. Therefore, we included the icosahedral components in Table 4 and the rms distance defined by

$$d_{\text{rms}} = \sqrt{\sum_{i=1}^6 (\sigma_{i,q,ch} - \sigma_{i,i,m})^2 / 6}. \quad (8)$$

The rms distances in Table 4 show that the full tensors  $\sigma_{i,m}^{(k)}$  and  $\sigma_{q,ch}^{(k)}$  of all protons  $k$  in biphenyl agree within limits of 0.13–0.45 ppm. Systematic errors of our quantum chemical calculations are eliminated by comparing the isotropic shieldings referenced to the *para* values. By this strategy we remove in particular those systematic errors which are inherent to the methodology, including basis set incompleteness, and the neglect of rovibrational contributions. Also, when discussing traceless principal values or traceless icosahedral tensors, systematic errors are reduced considerably.

Theory and experiment also agree in that at all sites *para*, *meta*, and *ortho* in biphenyl the *asymmetry* of the proton shielding is nearly maximal, see again Table 4. Nevertheless, a trend can be observed:  $\sigma_{22,i,m}$  as well as  $\sigma_{22,q,ch}$  decreases from *para*  $\Rightarrow$  *meta*  $\Rightarrow$  *ortho*, for the *ortho* proton  $\sigma_{22,q,ch}$  is even negative. A significant trend *para*  $\Rightarrow$  *meta*  $\Rightarrow$  *ortho* exists also in the shielding *anisotropy* and, as already discussed, in the deviation  $\varepsilon_{im}$ . All these trends including that of the isotropic shieldings can readily be rationalized by considering the second aromatic ring of the biphenyl molecule as a ‘neighbour molecule’ of that ring whose protons are in the focus of interest.

Before closing we briefly return to the initial motivation of this work, which was interest in the proton shielding in benzene, and to the closing-down of the line-narrowing multiple pulse technique. The results of this work imply beyond any reasonable doubt that in the *isolated* benzene molecule the C–H bond direction is the *intermediate* principal proton shielding direction. In a benzene *crystal*, no principal shielding direction can be expected to point along the bond direction. The present work suggests, moreover, that in a benzene crystal the relation between C–H bond and orientation of proton shielding tensor is substantially different for the three crystallographically non-equivalent protons of the molecule. The powder spectrum of benzene that in principle can be observed at a temperature low enough for molecular jumps to have frozen out, will necessarily be the superposition of three independent powder spectra—and thus would defy any detailed analysis. Recall that the powder spectrum of benzene reported by Ryan et al. [5] was recorded at  $-50$  °C where reorientational jumps are still frequent.

In the Introduction we explained why a single-crystal line-narrowing multiple pulse experiment on benzene with immobile molecules is close to impossible. The good news of this work is that there is no more a need to perform such an experiment. Actually, proton shielding tensors are hardly anymore a reason to perform line-narrowing multiple pulse experiments. There are adequate,

even superior, alternatives: first, single crystal deuteron NMR in very high applied fields [16] and, second, calculation by the quantum chemical method explored and tested against experiment here, perhaps supplemented by the old susceptibility method. After elimination of systematic errors, these theoretical methods allow with reasonable effort to access proton shielding tensors on a sub-ppm accuracy level not only in the isolated molecule but also in the natural crystal environment. In a forthcoming publication we shall give a fuller account of these methods and shall apply them to benzene (T. Heine, C. Corminboeuf, G. Grossmann, U. Haeberlen).

## Acknowledgments

Writing up this work was stimulated by a talk of O.L. Malkina and V.G. Malkin presented in late summer 2003 at the EMBL in Heidelberg, Germany. We thank Prof. G. Seifert from the Chemistry Department of the University of Dresden for inspiring discussions and continuous support, and Manfred Hauswirth from the mechanical shop of the MPI in Heidelberg for making, under a magnifying CCD camera, the delicate parts shown in Fig. 2 including the nearly spherical sample crystal. We gratefully acknowledge financial support from the Deutsche Forschungsgemeinschaft (DFG) and the Swiss NFS, grant 200020.100070/1.

## References

- [1] J.S. Waugh, L.M. Huber, U. Haeberlen, Approach to high-resolution NMR in solids, *Phys. Rev. Lett.* 20 (1968) 180–182.
- [2] U. Haeberlen, High Resolution NMR in Solids, Selective Averaging, *Advances in Magnetic Resonance*, Academic Press, New York, 1976, Suppl. 1.
- [3] U. Haeberlen, Multiple pulse techniques in solid state NMR, *Magn. Reson. Rev.* 10 (1985) 81–110, and references therein.
- [4] H.W. Spiess, H. Zimmermann, U. Haeberlen, Proton magnetic shielding and susceptibility effects in single crystals of ferrocene, *Chem. Phys.* 12 (1976) 123–130.
- [5] L.M. Ryan, R.C. Wilson, B.C. Gerstein, The proton magnetic shielding anisotropy in benzene, *J. Chem. Phys.* 67 (1977) 4310–4311.
- [6] S. Aravamudhan, U. Haeberlen, H. Irgartinger, C. Krieger, Pyromellitic acid dianhydride: crystal structure and anisotropic magnetic shielding, *Mol. Phys.* 38 (1979) 241–255.
- [7] P. Lazzeretti, M. Malagoli, R. Zanasi, Coupled Hartree–Fock calculations of magnetic properties of the benzene molecule: estimate of the Hartree–Fock limit for magnetic susceptibilities and nuclear magnetic shieldings, *J. Mol. Struct. (Theochem)* 80 (1991) 127–145.
- [8] K. Wolinski, J.F. Hinton, P. Pulay, Efficient implementation of the gauge-independent atomic orbital method for NMR chemical shift calculations, *J. Am. Chem. Soc.* 112 (1990) 8251–8260.
- [9] W. Kutzelnigg, U. Fleischer, M. Schindler, The IGLO-method: ab initio calculation and interpretation of NMR chemical shifts and magnetic susceptibilities, *NMR Basic Principles and Progress*, vol. 23, Springer-Verlag, Heidelberg, 1991, pp. 165–262.
- [10] D. Hoffmann, Ab initio Berechnungen der magnetischen Abschirmung von Protonen mit dem Programm RPAC, Diploma thesis (1990), University of Heidelberg.
- [11] F. Schönborn, Die Tensoren der magnetischen Abschirmung von Protonen in aromatischen Systemen, Diploma thesis (1996) University of Heidelberg.
- [12] G.P. Charbonneau, Y. Dëlugeard, Biphenyl: three-dimensional data and new refinement at 293 K, *Acta Cryst. B* 33 (1977) 1586–1588.
- [13] A. Müller, H. Zimmermann, U. Haeberlen, New aspects of spin diffusion and cross relaxation in solid-state NMR, *J. Magn. Reson.* 126 (1997) 66–78.
- [14] C. Meinel, H. Zimmermann, H. Schmitt, U. Haeberlen, Dynamics in molecular crystals: an application of proton NMR to selectively protonated biphenyl. Do the rings flip together or independently? *Appl. Magn. Reson.* 24 (2003) 25–40.
- [15] H. Post, U. Haeberlen, Proton shielding in single crystals of calcium and lead formate, *J. Magn. Reson.* 40 (1980) 17–31.
- [16] H. Schmitt, H. Zimmermann, O. Körner, M. Stumber, C. Meinel, U. Haeberlen, Precision measurement of the quadrupole coupling and chemical shift tensors of the deuterons in alpha-calcium formate, *J. Magn. Reson.* 151 (2001) 65–77.
- [17] D.H. Barich, R.J. Pugmire, D.M. Grant, R.J. Iulucci, Investigation of the structural conformation of biphenyl by solid-state  $^{13}\text{C}$  NMR and quantum chemical NMR shift calculations, *J. Phys. Chem. A* 105 (2001) 6780–6784.
- [18] G.-P. Charbonneau, Y. Dëlugeard, Structural transitions in polyphenyls. III. Crystal structure of biphenyl at 110 K, *Acta Cryst. B* 32 (1976) 1420–1423.
- [19] P.J.L. Baudour, Y. Dëlugeard, S. Ghémid, Transitions de phase structurales dans les Polyphényles. IX. Affinements des structures du *p*-terphényle hydrogéné à 200 K (diffraction des rayons X) et du biphényle Deutééré à 40 K (diffraction des neutrons), *Acta Cryst. C* C42 (1986) 1211–1217.
- [20] R. Prigl, U. Haeberlen, The theoretical and practical limits of resolution in multiple pulse high resolution NMR of solids, *Adv. Magn. Opt. Reson.* 19 (1996) 1–58.
- [21] D.P. Burum, W.K. Rhim, Analysis of multiple pulse NMR in solids III, *J. Chem. Phys.* 71 (1979) 944–956.
- [22] B. Tesche, U. Haeberlen, Proton chemical-shift tensors of methyl groups: a multiple-pulse NMR and LORG/IGLO ab initio study, *J. Magn. Reson. A* 117 (1995) 186–192.
- [23] Gaussian 98, Revision A.7, M.J. Frisch, G.W. Trucks, H.B. Schlegel, G.E. Scuseria, M.A. Robb, J.R. Cheeseman, V.G. Zakrzewski, J.A. Montgomery, Jr., R.E. Stratmann, J.C. Burant, S. Dapprich, J.M. Millam, A.D. Daniels, K.N. Kudin, M.C. Strain, O. Farkas, J. Tomasi, V. Barone, M. Cossi, R. Cammi, B. Mennucci, C. Pomelli, C. Adamo, S. Clifford, J. Ochterski, G.A. Petersson, P.Y. Ayala, Q. Cui, K. Morokuma, D.K. Malick, A.D. Rabuck, K. Raghavachari, J.B. Foresman, J. Cioslowski, J.V. Ortiz, A.G. Baboul, B.B. Stefanov, G. Liu, A. Liashenko, P. Piskorz, I. Komaromi, R. Gomperts, R.L. Martin, D.J. Fox, T. Keith, M.A. Al-Laham, C.Y. Peng, A. Nanayakkara, C. Gonzalez, M. Challacombe, P.M.W. Gill, B. Johnson, W. Chen, M.W. Wong, J.L. Andres, C. Gonzalez, M. Head-Gordon, E.S. Replogle, and J.A. Pople, Gaussian, Inc., Pittsburgh PA, (1998).
- [24] W. Kutzelnigg, Theories of magnetic susceptibilities and NMR chemical shifts in terms of localized quantities, *Isr. J. Chem.* 19 (1980) 193–200.
- [25] S.F. Boys, Construction of some molecular orbitals to be approximately invariant for changes from one molecule to another, *Rev. Mod. Phys.* 32 (1960) 296–299; J.M. Foster, S.F. Boys, Canonical configurational interaction procedure, *Rev. Mod. Phys.* 32 (1960) 300–302.
- [26] J.P. Perdew, K. Burke, M. Ernzerhof, Generalized gradient approximation made simple, *Phys. Rev. Lett.* 77 (1996) 3865–3868.

- [27] A.M. Köster, R. Flores, G. Geudtner, A. Goursot, T. Heine, S. Patchkovskii, U.R. Reveles, A. Vela, D.R. Salahub deMon, NRC Ottawa, Canada, (2004).
- [28] V.G. Malkin, O.L. Malkina, D.R. Salahub deMon-NMR, NRC Ottawa, Canada, (2004).
- [29] F. Tran, J. Weber, T.A. Wesolowski, Theoretical study of the benzene dimer by the density-functional-theory formalism based on electron-density partitioning, *Helv. Chim. Acta* 84 (2001) 1489–1503.
- [30] T. Heine, L. Zhechkov, G. Seifert, Hydrogen storage by physisorption on nanostructured graphite platelets, *Phys. Chem. Chem. Phys.* 6 (2004) 980–984.
- [31] G. Merino, T. Heine, G. Seifert, The induced magnetic field in cyclic molecules, *Chem. Eur. J.* 10 (2004) 4367–4371.
- [32] See Eq. 2.49 of p.18 of M. Mehring, High resolution NMR spectroscopy in solids, in: P. Diehl, E. Fluck, R. Kosfeld (Eds.), *NMR Basic Principles and Progress*, vol. 11, Springer-Verlag, Heidelberg, 1976.
- [33] H.M. McConnell, Theory of nuclear magnetic shielding in molecules. I. Long-range dipolar shielding of protons, *J. Chem. Phys.* 27 (1957) 226–229.
- [34] U. Haeberlen, J.S. Waugh, Spin lattice relaxation in periodically perturbed systems, *Phys. Rev.* 185 (1969) 420–429.
- [35] P. Blustin, A localized  $\pi$ -bond model for the calculation of molar magnetic susceptibilities and anisotropies of aromatic hydrocarbons, *Mol. Phys.* 36 (1978) 1441–1448.
- [36] Landold-Börnstein, *Magnetic Properties II*, vol. II, part 10, Springer-Verlag, Heidelberg, 1967, p. 115.
- [37] D.W. Alderman, M.H. Sherwood, D.M. Grant, Comparing, modeling, and assigning chemical-shift tensors in the Cartesian, irreducible spherical, and icosahedral representations, *J. Magn. Reson. A* 101 (1993) 188–197.